

## M multinuclear Solid-state NMR Investigation of Nanoporous Silica Prepared by Sol-gel Polymerization Using Sodium Silicate

Sun Ha Kim,<sup>†</sup> Oc Hee Han,<sup>†,‡,\*</sup> Jong Kil Kim,<sup>§</sup> and Kwang Ho Lee<sup>§</sup>

<sup>†</sup>Daegu Center, Korea Basic Science Institute, Daegu 702-701, Republic of Korea

<sup>‡</sup>Graduate School of Analytical Science & Technology, Chungnam National University, Daejeon 305-764, Republic of Korea

\*E-mail: ohhan@kbsi.re.kr

<sup>§</sup>E&B Nanotech Co. Ltd, Gyeonggido 426-901, Republic of Korea

Received June 20, 2011, Accepted August 11, 2011

M multinuclear solid-state nuclear magnetic resonance (NMR) experiments were performed to investigate the local structure changes of nanoporous silica during hydrothermal treatment and surface modification with 3-aminopropyltriethoxysilane (3-APTES). The nanoporous silica was prepared by sol-gel polymerization using inexpensive sodium silicate as a silica precursor. Using <sup>1</sup>H magic angle spinning (MAS) NMR spectra, the hydroxyl groups, which play an important role in surface reactions, were probed. Various silicon sites such as Q<sup>2</sup>, Q<sup>3</sup>, Q<sup>4</sup>, T<sup>2</sup>, and T<sup>3</sup> were identified with <sup>29</sup>Si cross polarization (CP) MAS NMR spectra and quantified with <sup>29</sup>Si MAS NMR spectra. The results indicated that about 25% of the silica surface was modified. <sup>1</sup>H and <sup>29</sup>Si NMR data proved that the hydrothermal treatment induced dehydration and dehydroxylation. The <sup>13</sup>C CP MAS and <sup>1</sup>H MAS NMR spectra of 3-APTES attached on the surface of nanoporous silica revealed that the amines of the 3-aminopropyl groups were in the chemical state of NH<sub>3</sub><sup>+</sup> rather than NH<sub>2</sub>.

**Key Words :** Silica, Nuclear magnetic resonance, MAS NMR, Surface functionalization

### Introduction

Nanoporous silica materials with high surface area have been utilized as fillers in elastomeric materials such as tires, thermal and acoustic insulators, low k materials, adsorbents, separators, censors, filters for exhaust gases, and heterogeneous catalysts in various chemical reactions.<sup>1-5</sup> Silica is the most highly porous nanostructured material currently available, and has a large surface area, high porosity, and low bulk density.<sup>6</sup> In contrast with silica prepared with expensive alkoxides like tetraethoxysilane (TEOS),<sup>7</sup> our silica can be prepared in mass production for use in the industry by sol-gel polymerization of inexpensive sodium silicate precursor and dried at atmospheric pressure for green chemistry. Furthermore, considering the application of silica for elastomeric materials, the silica was hydrothermally treated to control its textural properties such as surface area, pore volume, and pore size. The silica surface was then modified by coupling hydroxyl groups on the surface with an organoalkoxysilane such as 3-aminopropyltriethoxysilane (3-APTES).<sup>8</sup> The ability of this aminoalkoxysilane-functionalized silica to be easily dispersed in organic materials such as rubber opened up extensive opportunities for use as a filler for rubber in the tire industry.

Solid-state nuclear magnetic resonance (NMR) spectroscopy is an excellent tool to investigate local structures of nanoporous silica materials and dynamics of protons on nanoporous silica.<sup>9-11</sup> In this work, <sup>1</sup>H, <sup>29</sup>Si, and <sup>13</sup>C solid-state NMR spectroscopy was used to investigate surface reactions on the silica materials during hydrothermal treatment and surface functionalization with 3-APTES.

### Experimental

**Preparation of Silica.** Pure silica was prepared by sol-gel polymerization using a sodium silicate (Shinwoo Materials Co. Ltd., Republic of Korea) with a molar ratio of SiO<sub>2</sub>:Na<sub>2</sub>O = 3.4:1. The preparation method used to prepare the nanoporous silica at an ambient pressure is schematically shown in Figure 1. For preparing the silica sol, the aqueous sodium silicate solution (SiO<sub>2</sub> = 24%) was mixed with sulfuric acid solution (40%) through a line mixer (by nozzle) as shown in Figure 1. Then the acidic (pH ~ 1) silica sol was

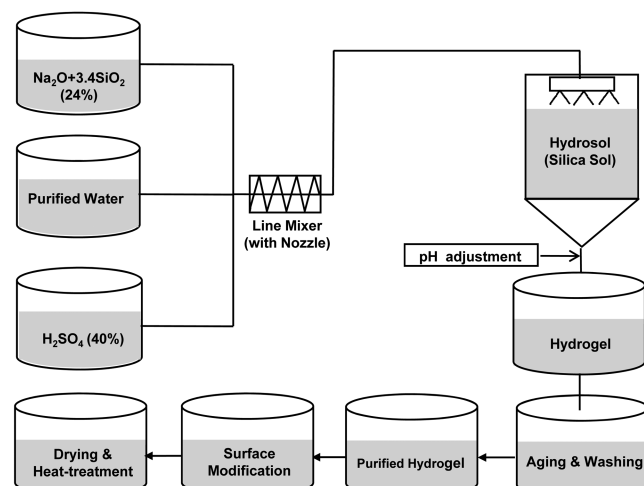


**Figure 1.** Schematic of the experimental procedure for the synthesis of hydrophobic and hydrophilic nanoporous silica with sodium silicate precursor at ambient pressure.

collected in a gelation unit prior to gelation. The gelation took only about 4 minutes due to the high silica concentration in the silica sol solution and the strongly acidic pH. After gelation, the resultant silica was aged at a predetermined pH and temperature. The prepared silica was thoroughly washed with a continuous flow of water for 12 hours to remove trapped sodium ions ( $\text{Na}^+$ ) from the wet silica. The removal of  $\text{Na}^+$  from the washed gel was confirmed by a sodium ion detector (NeoMet, ISTEK, Republic of Korea). For silica with large pore sizes, the as-synthesized silica was hydrothermally treated by heating at 180 °C in the presence of water for 2 hour. To introduce amino-groups onto the silica surface, 100 g of silica (150-425 mesh) was suspended in 350 mL of water, while 3-APTES (10%) and hydrochloric acid solution (HCl, 10%) were simultaneously added. The reaction pH of the mixture was maintained between 3 and 3.5 and the final pH was maintained at 3.5. After the addition of 3-APTES, the reaction mixture was aged at 80 °C for 2 hours. Finally, the functionalized silica was dried at 75 °C for 2 hours and at 125 °C for 2 hours.

**Solid-state NMR Experiments.** The  $^1\text{H}$ ,  $^{29}\text{Si}$ , and  $^{13}\text{C}$  NMR spectra were obtained using a Bruker DSX 400 MHz spectrometer at 9.4 T at Larmor frequencies of 400.13, 79.49, and 100.62 MHz, respectively, and at spinning rates of 14, 6 and 6 kHz, respectively, by using 4 mm zirconia rotors. All  $^1\text{H}$  magic angle spinning (MAS) NMR spectra were acquired using one pulse sequence with a pulse repetition delay of 3 s and an excitation pulse length of 2  $\mu\text{s}$  corresponding to a 45° flip of magnetization.  $^{29}\text{Si}$  and  $^{13}\text{C}$  cross polarization (CP) MAS NMR spectra for qualitative analyses were acquired with a pulse repetition delay of 3 s, a contact time of 2 ms, and a proton excitation pulse length of 4  $\mu\text{s}$  for  $^{29}\text{Si}$  and of 4.2  $\mu\text{s}$  for  $^{13}\text{C}$ .  $^{29}\text{Si}$  MAS NMR spectra for quantitative analyses were acquired using a single pulse sequence with a pulse repetition delay of 100 s, an excitation pulse length of 1.5  $\mu\text{s}$ , and proton decoupling with  $\text{H}_1$  field strength of 62.5 kHz. For comparison with the spectra of surface-functionalized silica,  $^{13}\text{C}$  and  $^{29}\text{Si}$  NMR spectra of neat 3-APTES liquid in a rotor were obtained using a single pulse sequence under proton decoupling in non-spinning condition. The chemical shifts were referenced against tetramethylsilane.

## Results and Discussion

**Physical Properties of Silica.** For as-synthesized silica, a Brunauer-Emmett-Teller (BET) surface of 840.37  $\text{m}^2/\text{g}$ , a pore volume of 0.23  $\text{cm}^3/\text{g}$ , and a pore size of 28.97 Å were obtained. The hydrothermally treated silica had a BET surface area of 152.17  $\text{m}^2/\text{g}$ , a pore volume of 1.08  $\text{cm}^3/\text{g}$ , and a pore size of 318.30 Å. The surface-functionalized silica had a BET surface area of 384.06  $\text{m}^2/\text{g}$ , a pore volume of 1.14  $\text{cm}^3/\text{g}$ , and a pore size of 115.68 Å. The BET surface area was drastically reduced by hydrothermal treatment but increased by surface functionalization. The pore volume was drastically increased by hydrothermal treatment and slightly increased by surface functionalization. The pore size was

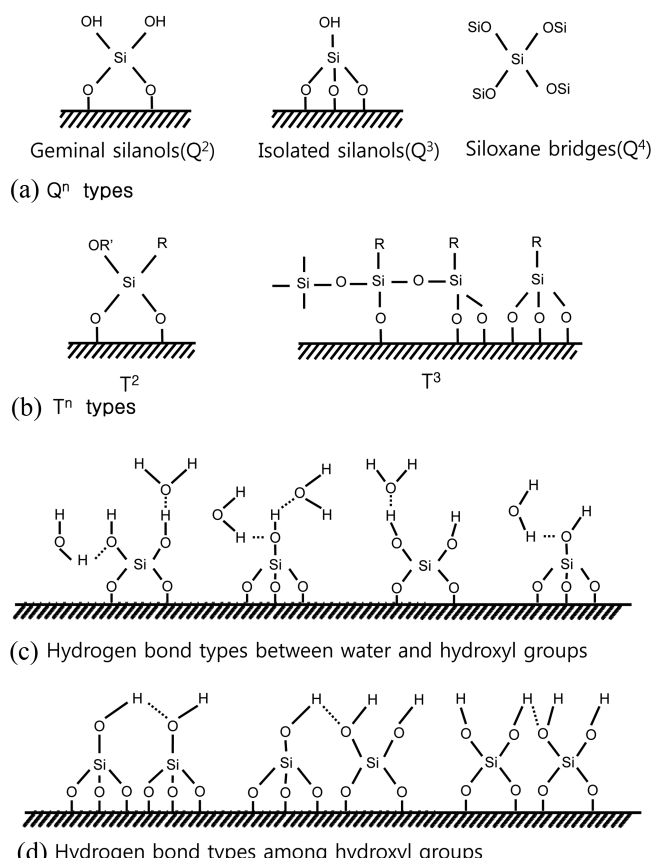


**Figure 2.** Various types of silicon units in silica: (a)  $\text{Q}^n$  types, (b)  $\text{T}^n$  types, (c) hydrogen bond types between waters and hydroxyl groups, and (d) hydrogen bond types among hydroxyl groups.

drastically increased by hydrothermal treatment and decreased by surface functionalization.

**$^1\text{H}$  MAS NMR.** The hydroxyl groups in silica are known to be present as isolated hydroxyl groups, geminal hydroxyl groups, and hydrogen-bonded forms,<sup>12-14</sup> and the hydrogen bonds can be formed among hydroxyl groups or between hydroxyl groups and water,<sup>12,15,16</sup> as schematically summarized in Figure 2.

Figure 3(a) shows a representative  $^1\text{H}$  MAS NMR spectrum of the as-synthesized silica. The spectrum was deconvoluted to peaks at 1.8, 2.1, 3.1 and 4.7 ppm, for which the first two peaks were assigned to isolated hydroxyl groups and geminal hydroxyl groups, respectively.<sup>9,17</sup> The signal at 3.1 ppm was interpreted as the hydroxyl groups hydrogen-bonded with water while the broad signal at 4.7 ppm was assigned to the hydroxyl groups hydrogen-bonded with the hydroxyl groups.<sup>15,16,18</sup> Thus isolated hydroxyl groups, geminal hydroxyl groups, hydroxyl groups hydrogen-bonded with water, and hydroxyl groups hydrogen-bonded with hydroxyl groups were present on the surface of the as-synthesized silica. Figure 3(b) presents a representative  $^1\text{H}$  MAS NMR spectrum of the hydrothermally treated silica and the deconvoluted spectrum was used to generate the peaks of isolated hydroxyl groups at 1.8 ppm, geminal hydroxyl groups at 2.1 ppm, and hydroxyl groups hydrogen-

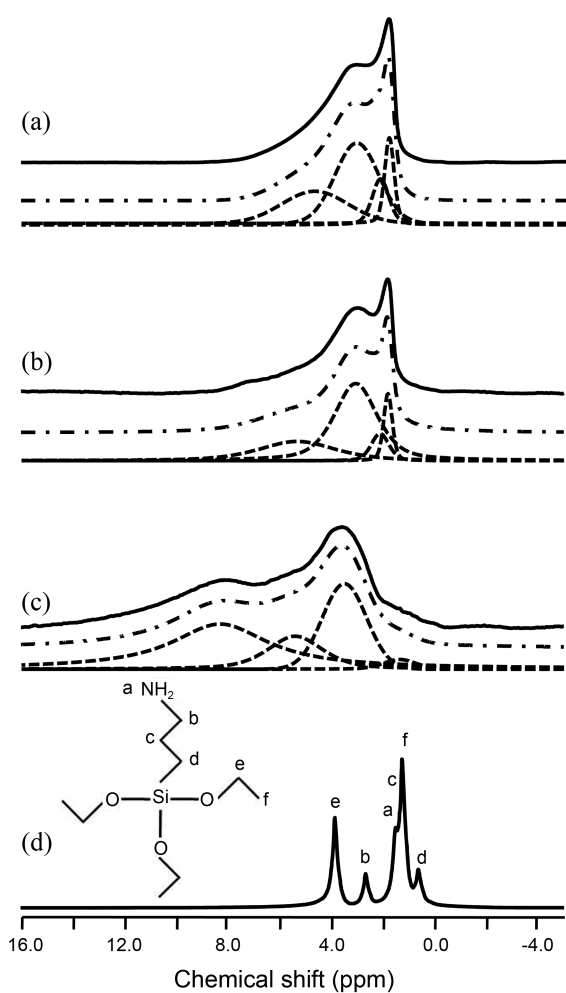


**Figure 3.**  $^1\text{H}$  MAS NMR spectra of the (a) as-synthesized silica, (b) hydrothermally treated silica, (c) surface-functionalized silica, and (d) 3-APTES. The lines of —, -·-, and -·— represent the experimental spectra, sum of the respective deconvoluted peaks, and respective deconvolution peaks, respectively. The letters in Figure 3(d) represent the positions of the respective hydrogens.

bonded with water at 3.1 ppm. The chemical shift values of the peaks were identical with those of the peaks observed with the as-synthesized silica. However, the total hydrogen signal was reduced to 15% of that of the as-synthesized silica as summarized in Table 1. This reduction of the total hydrogen signal was attributed to the removal of some hydroxyl groups on the surface silica by dehydration and dehydroxylation that occurred during hydrothermal treat-

ment. In terms of the relative population of each peak, the intensities of the isolated hydroxyl groups at 1.8 ppm and geminal hydroxyl groups at 2.1 ppm were reduced while the signal at 3.1 ppm for hydroxyl groups hydrogen-bonded with water was slightly increased. Moreover, the signals for hydroxyl groups hydrogen-bonded with hydroxyl groups were shifted from 4.7 ppm to 5.3 ppm and the linewidth of the signal became slightly broader. These increased chemical shifts and broadened linewidth were attributed to the stronger hydrogen bonding induced by the reduced number of hydroxyl groups involved in hydrogen bonding. The number of hydroxyl groups was reduced due to the hydrothermal treatment. Therefore, this hydrothermal treatment-induced change of the silica surface is expected to influence the macro properties of the silica.<sup>19</sup>

After the hydrothermally treated silica was functionalized by 3-APTES, signals of the isolated hydroxyl groups at 1.8 ppm and geminal hydroxyl groups at 2.1 ppm almost disappeared, as shown in Figure 3(c). However, the signal observed at 3.1 ppm for the hydroxyl groups hydrogen-bonded with water in the hydrothermally treated silica was shifted to 3.5 ppm and exhibited an increased intensity. This signal shift was explained by the interaction of NH<sub>3</sub><sup>+</sup> with the hydroxyl groups hydrogen-bonded with water via proton exchange directly and/or through water. In addition, a new, large and broad signal appeared at 8.3 ppm as well as a very small signal at 1.3 ppm. From chemical shift analysis using ChemDraw ultra 9.0 software and the comparison with the spectrum of 3-APTES in Figure 3(d), the former was verified as NH<sub>3</sub><sup>+</sup> generated from NH<sub>2</sub> at the tail of 3-APTES on silica surface and the latter as hydrogens of Si-CH<sub>2</sub>CH<sub>2</sub>-attached on the silica surface. The relatively large intensity of the former compared to the stoichiometric intensity of the latter implies hydrogen bonding between NH<sub>3</sub><sup>+</sup> and water.

**$^{29}\text{Si}$  CP MAS NMR.** Structural elements of silica consist of SiO<sub>4</sub> units without any hydroxyl groups attached (Q<sup>4</sup>) and silanol groups units with hydroxyl groups such as Q<sup>1</sup>, Q<sup>2</sup>, and Q<sup>3</sup>. In addition, the attachment of organic species on the surface results in T<sup>1</sup>, T<sup>2</sup> and T<sup>3</sup> units.<sup>20,21</sup> In Figure 4(a), the peaks of Q<sup>2</sup>, Q<sup>3</sup>, and Q<sup>4</sup> units in the as-synthesized silica appeared at -91 ppm, -100 ppm, and -110 ppm, respectively.<sup>21,22</sup> After the hydrothermal treatment, the signals for the Q<sup>2</sup> and Q<sup>4</sup> units were decreased and enhanced, respectively, as shown in Figure 4(b), indicating the dehydroxylation of the Q<sup>2</sup> and Q<sup>3</sup> units to generate the Q<sup>3</sup> and Q<sup>4</sup> units.

After the hydrothermally treated silica was functionalized

**Table 1.** Chemical shift and total peak area of  $^1\text{H}$  MAS NMR spectra

Samples	Chemical shift (ppm)					Total peak area for each sample <sup>a</sup> (%)
	Isolated hydroxyl group	Geminal hydroxyl group	Hydroxyl groups hydrogen-bonded with water	Hydroxyl groups hydrogen-bonded with hydroxyl groups	NH <sub>3</sub> <sup>+</sup> on the surface-functionalized silica	
As-synthesized silica	1.8	2.1	3.1	4.7	-	100
Hydrothermally treated silica	1.8	2.1	3.1	5.3	-	15
Surface functionalized silica	1.8	2.1	3.5	5.3	8.3	24

<sup>a</sup>Total peak area was obtained for each sample and compared to that of the as-synthesized silica.

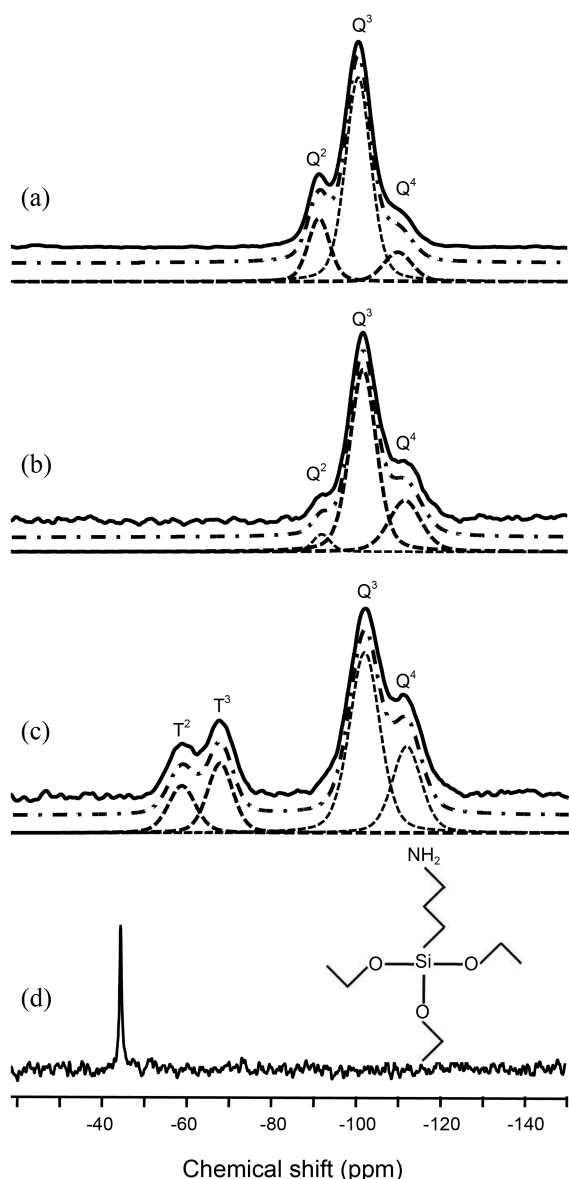


**Figure 4.**  $^{29}\text{Si}$  CP MAS NMR spectra of the (a) as-synthesized silica, (b) hydrothermally treated silica, (c) surface-functionalized silica, and (d)  $^{29}\text{Si}$  liquid NMR spectrum of neat 3-APTES. Q<sup>2</sup>, Q<sup>3</sup>, Q<sup>4</sup>, T<sup>2</sup>, and T<sup>3</sup> are defined in Figure 2 and in the main text. The lines of —, ——, and - - - represent the experimental spectra, sum of the respective deconvoluted peaks, and respective deconvolution peaks, respectively.

by 3-APTES, the signals of the Q<sup>2</sup> units at -91 ppm almost disappeared and the signals of the Q<sup>3</sup> units at -100 ppm decreased. However, the signal of the Q<sup>4</sup> units at -110 ppm increased, as shown in Figure 4(c). In addition, the signals of the T<sup>2</sup> and T<sup>3</sup> units appeared at -58.6 and -67.7 ppm, respectively<sup>21</sup> while the  $^{29}\text{Si}$  NMR signal for neat 3-APTES appeared as a single peak at -50 ppm, as shown in Figure 4(d). Thus, the new appearance of these T<sup>2</sup> and T<sup>3</sup> units confirmed that the silica surface was functionalized by 3-APTES and that the modifiers were attached mostly to the Q<sup>2</sup> units and partially to the Q<sup>3</sup> units on the silica surface.

**$^{29}\text{Si}$  MAS NMR.** In order to analyze the  $^{29}\text{Si}$  NMR data

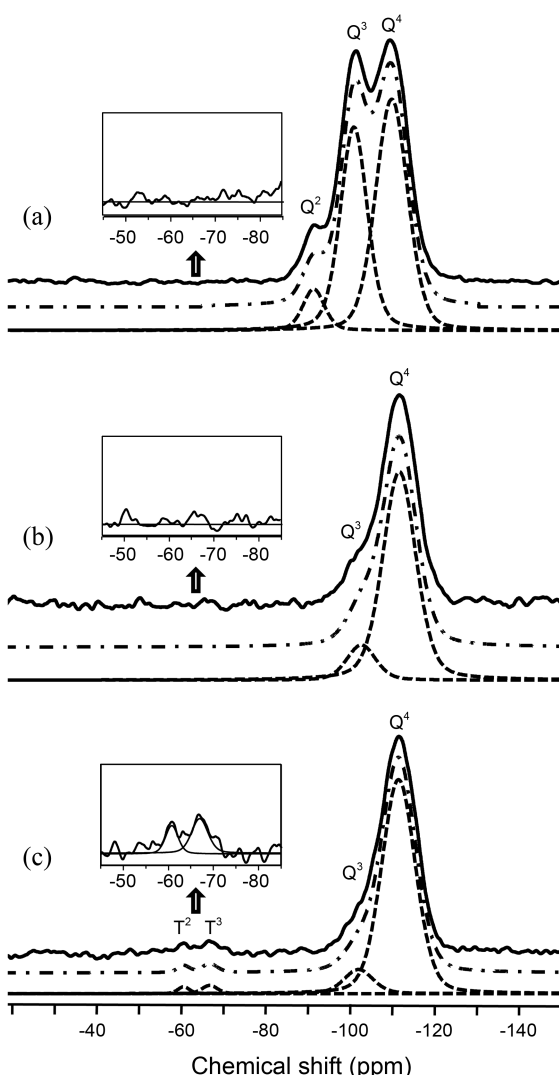


**Figure 5.**  $^{29}\text{Si}$  MAS NMR spectra of the (a) as-synthesized silica, (b) hydrothermally treated silica, and (c) surface-functionalized silica. Q<sup>2</sup>, Q<sup>3</sup>, Q<sup>4</sup>, T<sup>2</sup>, and T<sup>3</sup> are defined in Figure 2 and in the main text. The lines of —, ——, and - - - represent the experimental spectra, sum of the respective deconvoluted peaks, and respective deconvolution peaks, respectively.

for quantitative information on the structural units in silica,  $^{29}\text{Si}$  MAS NMR spectra were acquired and deconvoluted as shown in Figure 5, while the  $^{29}\text{Si}$  CP MAS NMR spectra were used for qualitative or semi-qualitative information. The peak-area ratio of the Q<sup>2</sup>, Q<sup>3</sup>, and Q<sup>4</sup> units in the as-synthesized silica was 6:41:53, as summarized in Table 2. This ratio indicates that the as-synthesized silica was mostly composed of isolated silanol groups (Q<sup>3</sup>) and SiO<sub>4</sub> units without any hydroxyl groups attached (Q<sup>4</sup>), and that some geminal silanols groups (Q<sup>2</sup>) were present as a minor component. Hydrothermal treatment of the as-synthesized silica almost completely removed the signal of the Q<sup>2</sup> unit (Figure 5(b)) and the peak-area ratio of Q<sup>3</sup> and Q<sup>4</sup> was changed to 13 and 87, as presented in Table 2. Therefore, as explained semi-quantitatively with the  $^{29}\text{Si}$  CP MAS NMR data, hydrothermal treatment induced dehydroxylation of the Q<sup>2</sup>

**Table 2.** Relative peak area obtained from deconvolution of  $^{29}\text{Si}$  MAS NMR spectra

Samples	$\text{T}^2$ (%)	$\text{T}^3$ (%)	$\text{Q}^2$ (%)	$\text{Q}^3$ (%)	$\text{Q}^4$ (%)
As-synthesized silica	-	-	6	41	53
Hydrothermally treated silica	-	-	-	13	87
Surface functionalized silica	1	2	-	9	88

<sup>a</sup>For each sample, the sum of the peak areas was adjusted to 100%.

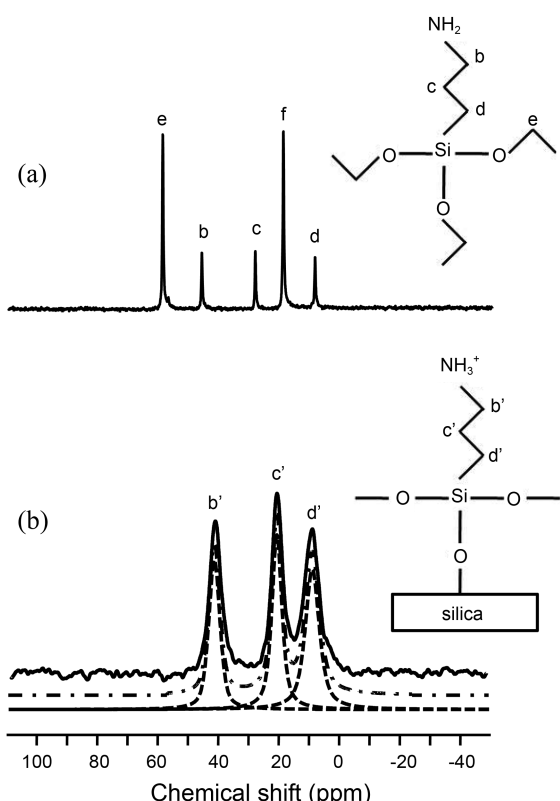


**Figure 6.** (a)  $^{13}\text{C}$  CP MAS NMR spectrum of the surface functionalized silica and (b)  $^{13}\text{C}$  liquid NMR spectrum of neat 3-APTES. The lines of —, ---, and - - - represent the experimental spectra, sum of the respective deconvoluted peaks, and respective deconvoluted peaks, respectively. The letters represent the positions of the respective carbons.

and  $\text{Q}^3$  units, thereby leading to the generation of  $\text{Q}^3$  and  $\text{Q}^4$  units. Figure 5(c) shows the  $^{29}\text{Si}$  MAS NMR spectrum for the surface-functionalized samples. The peak-area ratio was  $\text{T}^2:\text{T}^3:\text{Q}^3:\text{Q}^4 = 1:2:9:88$ , as presented in Table 2. Comparison of the peak ratio with that of the hydrothermally treated silica suggests that all of the surface functionalization occurred on the  $\text{Q}^3$  units, as expected, while the  $-\text{OCH}_2\text{CH}_3$  moieties of 3-APTES were removed as  $\text{HOCH}_2\text{CH}_3$  by reacting with the hydroxyl groups of the  $\text{Q}^3$  units. If all the silanol groups are assumed to be surface functionalization sites, the coverage of the surface modifier for functionalized silica can be calculated as  $\Sigma \text{T}^n / (\Sigma \text{T}^n + \Sigma \text{Q}^n)$  for  $n = 1, 2$ , and 3. For our surface-functionalized silica,  $\Sigma \text{T}^n / (\Sigma \text{T}^n + \Sigma \text{Q}^n) = (1+2)/(1+2+9) = 0.25 (\pm 0.08)$ .

**$^{13}\text{C}$  NMR.** To identify the chemical structure of organic modifiers on the silica surface, the  $^{13}\text{C}$  NMR spectra of the

modifier itself, 3-APTES, and of the surface-functionalized silica with 3-APTES were acquired. The signals of 3-APTES appeared at 59, 46, 28, 19, and 8.6 ppm, as shown in Figure 6(a), while the signals of the surface-functionalized silica appeared at 41, 21, and 8.6 ppm, as shown in Figure 6(b). The peaks at 59 and 19 ppm of the ethoxy carbons of 3-APTES disappeared after removal of the ethoxy groups as ethanol during surface functionalization. The peaks of propylamine carbons of 3-APTES were shifted from 46 and 28 ppm to 41 and 21 ppm signals, respectively, as shown in Figure 6(b), which may have resulted from the new chemical bonding of Si in 3-APTES with silanols on the silica surface and removal of ethoxy groups. However, the chemical shift of propylamine carbons would have been more strongly influenced by the chemical states of amines of propylamines due to the shorter chemical bonding distances to the nitrogens of the amines. The absence of any chemical shift change of the carbon signal at 8.6 ppm upon surface functionalization supports this latter argument. Indeed, simulation of chemical shifts agreed better with  $\text{NH}_3^+$  than  $\text{NH}_2$  for the amine groups of propylamines on the surface-functionalized silica.

## Conclusions

Nanoporous silica was prepared by sol-gel polymerization using inexpensive sodium silicate as a silica precursor. The silica was hydrothermally treated and sequentially functionalized with 3-APTES for better dispersion as a filler in elastomers used for automobile tires. The physical properties such as pore volume, pore size, and surface area of silica at each preparation state were measured.

$^1\text{H}$ ,  $^{29}\text{Si}$ , and  $^{13}\text{C}$  solid-state NMR spectra were acquired for the as-synthesized silica, hydrothermally treated silica, and surface-functionalized silica. The  $^1\text{H}$  MAS NMR data identified isolated hydroxyl groups, geminal hydroxyl groups, and hydroxyl groups hydrogen-bonded with water or other hydroxyl groups on the surface of the silica samples.  $\text{T}^2$ ,  $\text{T}^3$ ,  $\text{Q}^2$ ,  $\text{Q}^3$ , and  $\text{Q}^4$  units were identified from the results of the  $^{29}\text{Si}$  MAS and CP MAS NMR experiments. Observation of  $\text{T}^2$  and  $\text{T}^3$  ensured the surface functionalization. The  $^{29}\text{Si}$  MAS NMR spectra revealed that the surface coverage by the surface modifier was  $\sim 25\%$ . The  $^1\text{H}$  and  $^{29}\text{Si}$  NMR data confirmed the occurrence of dehydroxylation and dehydration during hydrothermal treatment. Comparative analysis of pure 3-APTES and 3-APTES attached on the silica by  $^{13}\text{C}$  NMR experiments confirmed that the conversion of the amine groups of the 3-aminopropyl groups from  $\text{NH}_2$  to  $\text{NH}_3^+$ .

**Acknowledgments.** This work was supported by the Technology Innovation Support Program [PB9009 and PB8026] granted to O. H. Han.

## References

- Pajonk, G. M. *Appl. Catal.* **1991**, 72, 217.
- Dias, A. S.; Pillinger, M.; Valente, A. A. *Micropor. Mesopor.*

- Mater.* **2006**, *94*, 214.
3. Jamali, M. R.; Aassadi, Y.; Shemirani, F.; Hosseini, M. R. M.; Kozani, R. R.; Masteri-Farahani, M.; Salavati-Niasani, M. *Anal. Chim. Acta* **2006**, *579*, 68.
  4. Tang, Q.; Xu, Y.; Wu, D.; Sun, Y. *J. Solid State Chem.* **2006**, *179*, 1513.
  5. Ren, Y.; Yue, B.; Gu, M.; He, H. *Mater.* **2010**, *3*, 764.
  6. Patel, R. P.; Purohit, N. S.; Suthar, A. M. *Int. J. ChemTech. Res.* **2009**, *1*, 1052.
  7. Hila, E.; David, A. *Chem. Mater.* **2008**, *20*, 2224.
  8. Iler, R. K. *The Chemistry of Silica*; Wiley: New York, 1979.
  9. Hartmeyer, G.; Marichal, C.; Lebeau, B.; Rigolet, S.; Caullet, P.; Hernandez, J. *J. Phys. Chem. C* **2007**, *111*, 9066.
  10. Brindle, R.; Pursch, M.; Albert, K. *Solid State Nucl. Magn. Reson.* **1996**, *6*, 251.
  11. Chuang, I.-S.; Kinney, D. R.; Maciel, G. E. *J. Am. Chem. Soc.* **1993**, *115*, 8695.
  12. Zhuravlev, L. T. *Colloids Surf. A* **2000**, *173*, 1.
  13. Dijkstra, T. W.; Duchateau, R.; van Santen, R. A.; Meetsma, A.; Yap, G. P. A. *J. Am. Chem. Soc.* **2002**, *124*, 9856.
  14. Jal, P. K.; Patel, S.; Mishra, B. K. *Talanta* **2004**, *62*, 1005.
  15. Grünberg, B.; Emmler, T.; Gedat, E.; Shenderovich, I.; Findenegg, G. H.; Limbach, H.-H.; Buntkowsky, G. *Chem. Eur. J.* **2004**, *10*, 5689.
  16. Yuan, P.; Wu, D.; Chen, Z.; Chen, Z.; Lin, Z.; Diao, G.; Peng, J. *Chin. Sci. Bull.* **2001**, *46*, 1128.
  17. van der Meer, J.; Bardez-Giboire, I.; Mercier, C.; Revel, B.; Davidson, A.; Denoyel, R. *J. Phys. Chem. C* **2010**, *114*, 3507.
  18. Dorémieux-Morin, C.; Heeribout, L.; Dumousseaux, C.; Fraissard, J.; Hommel, H.; Legrand, A. P. *J. Am. Chem. Soc.* **1996**, *118*, 13040.
  19. Stanislaus, A.; Al-Dolama, K.; Absi-Halabi, M. *J. Molec. Catal. A* **2002**, *181*, 33.
  20. Yasmin, T.; Müller, K. *J. Chromatogr. A* **2010**, *1217*, 3362.
  21. Albert, K. *J. Sep. Sci.* **2003**, *26*, 215.
  22. Lynch, B.; Glennon, J. D.; Tröltzsch, C.; Menyes, U.; Pursch, M.; Albert, K. *Anal. Chem.* **1997**, *69*, 1756.